PREDICTIVE MODELLING OF EXTRUSION-BASED 3D PRINTED PART PROPERTIES USING MACHINE LEARNING APPROACH

BTP report submitted
for the partial fulfillment of the requirements
for the degree of
Bachelor of Technology
By

KEERTI LATA (200103062)
ADITYA VERMA (200103007)

Under the guidance of Professor
Dr. BIRANCHI PANDA

DEPARTMENT OF MECHANICAL ENGINEERING

INDIAN INSTITUTE OF TECHNOLOGYGUWAHATI

(April 2024)

CERTIFICATE

This is to certify that the work contained in the project report titled “Predictive Modelling of Extrusion-Based 3d Printed Part Properties Using Machine Learning Approach” is a bonafide work of KEERTI LATA (200103062) and ADITYA VERMA (200103007) has been carried out in the Department of Mechanical Engineering, Indian Institute of Technology, Guwahati under my supervisionand that this work has not been submitted elsewhere for a degree.

DECLARATION

We declare that this written submission represents our ideas in our own words and where other's ideas or words have been included, we have adequately cited and referenced the original sources. We also declare that we have adhered to all principlesof academic honesty and integrity and have not misrepresented or fabricated or falsified any idea/data/fact/source in our submission. We understand that any violation of the above will be cause for disciplinary action by the Institute and can also evoke penal action from the sources which have thus not been properly cited or from whom proper permission has not been taken when needed.

Name: Keerti Lata
Roll No: 200103062
Department of Mechanical Eng.

Name: Aditya Verma
Roll No: 200103007
Department of Mechanical Eng.

APPROVAL SHEET

This project report entitled “Predictive Modelling of Extrusion-Based 3d Printed Part Properties Using Machine Learning Approach” by Aditya Verma (200103007) and Keerti Lata (200103062) is approved for the partial degree of Bachelor in Technology in Mechanical Engineering.

Examiners

_____

_____

_____

Supervisor (s)

_____

_____

_____

Chairman

_____

Date: 24-04-2023

Place: Guwahati

ACKNOWLEDGEMENT

We would like to express our earnest gratitude and respect to professor and project guide Dr. Biranchi Panda, for this project. We sincerely thank him for dedicating his valuable time in providing guidance, encouragement, support, and advice on various technical points during this project.

Name: Keerti Lata
Roll No: 200103062

Name: Aditya Verma
Roll No: 200103007

ABSTRACT

In the realm of additive manufacturing, understanding and optimizing the parameters affecting the mechanical properties of printed parts is crucial. This study focuses on investigating the Fused Deposition Modelling (FDM) process. The primary objective is to optimize input parameters to achieve desired levels of tensile strength in printed parts.
The research involves studying the effects of key parameters such as extruder temperature, number of contours, and layer thickness on the tensile strength of FDM-printed parts. Through systematic experimentation and tensile testing, data will be collected to analyse the influence of these variables.

Moreover, an AI model was developed to forecast the appropriate range of input parameters necessary to attain specific tensile strength targets. Two prominent machine learning techniques, Support Vector Machine (SVM) and Artificial Neural Network (ANN), were explored to ascertain the most suitable model for this predictive task.

The experimental data acquired from tensile tests served as the training dataset for the AI model. The model's performance was assessed by comparing its predictions with actual experimental results, thereby evaluating its accuracy in forecasting the optimal parameter ranges for desired tensile strength. The performance of the proposed two model is compared and it is found that the Support Vector Regression model (SVR) is better for solving this problem as compared to Artificial Neural Network (ANN).

This research aimed to contribute to the comprehension of FDM process optimization and furnish a practical tool for engineers and manufacturers to proficiently design and produce parts with desired mechanical properties.

CONTENTS

CHAPTER 1: INTRODUCTION

1.1 Background:

In recent decades, communications, imaging, architecture and engineering have all undergone their own digital revolutions. Now, AM can bring digital flexibility and efficiency to manufacturing operations.

Additive manufacturing uses data computer-aided-design (CAD) software or 3D object scanners to direct hardware to deposit material, layer upon layer, in precise geometric shapes. As its name implies, additive manufacturing adds material to create an object. By contrast, when you create an object by traditional means, it is often necessary to remove material through milling, machining, carving, shaping or other means.

Although the terms "3D printing" and "rapid prototyping" are casually used to discuss additive manufacturing, each process is actually a subset of additive manufacturing.

While additive manufacturing seems new to many, it has actually been around for several decades. In the right applications, additive manufacturing delivers a perfect trifecta of improved performance, complex geometries and simplified fabrication. As a result, opportunities abound for those who actively embrace additive manufacturing.

The term “additive manufacturing” references technologies that grow three-dimensional objects one superfine layer at a time. Each successive layer bonds to the preceding layer of melted or partially melted material. Objects are digitally defined by computer-aided-design (CAD) software that is used to create .stl files that essentially "slice" the object into ultra-thin layers. This information guides the path of a nozzle or print head as it precisely deposits material upon the preceding layer. Or, a laser or electron beam selectively melts or partially melts in a bed of powdered material. As materials cool or are cured, they fuse together to form a three-dimensional object.

In 2010, the American Society for Testing and Materials (ASTM) group “ASTM F42 – Additive Manufacturing”, formulated a set of standards that classify the range of Additive Manufacturing processes into 7 categories (Standard Terminology for Additive Manufacturing Technologies, 2012).

1. VAT Photopolymerization

2. Material Jetting

3. Binder Jetting

4. Material Extrusion

5. Powder Bed Fusion

6. Sheet Lamination

7. Directed Energy Deposition

In all of GE Additive's machines the process involves the spreading of the metal powder layer by layer and uses either a laser or electron beam to melt and fuse powder together to create a part. The process repeats until the entire part is created. Loose or unfused powder is removed during post processing and is recycled for the next build.

1.2 Fused Deposition Modelling:

- Fused Deposition Modeling (FDM), or Fused Filament Fabrication (FFF), is an additive manufacturing process that belongs to the material extrusion family. In FDM, an object is built by selectively depositing melted material in a pre-determined path layer-by-layer. The materials used are thermoplastic polymers and come in a filament form. Fishbone diagram to illustrate the main effect of process parameters is shown in Fig. 1.
- FDM is the most widely used 3D Printing technology. It represents the largest installed base of 3D printers globally and is often the first technology people are exposed to. In this article, the basic principles and the key aspects of the technology are presented. A basic model of FDM is shown in Fig. 2.

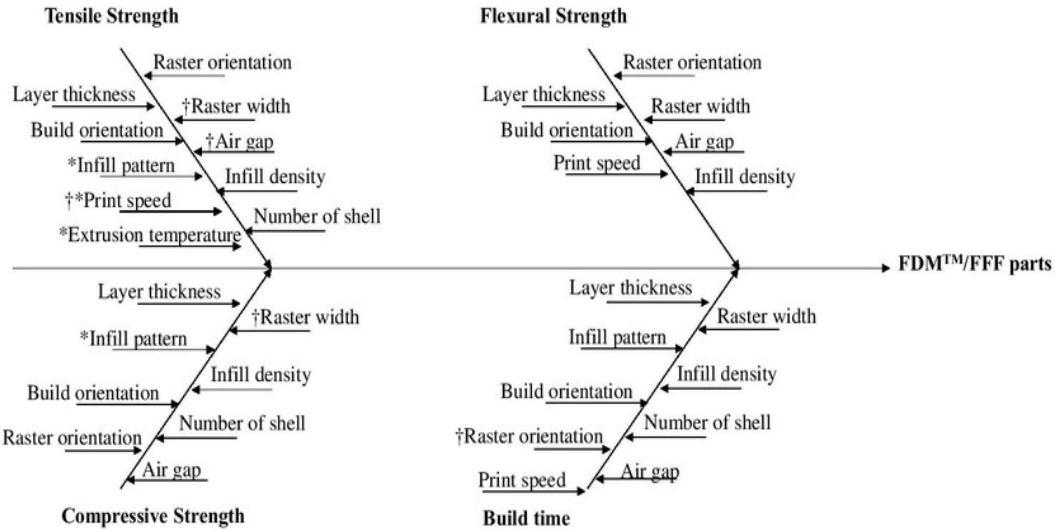

† Still unknown whether a parameter is significant or not
* Less analyzed compared to others

Fig.1. Fishbone diagram to illustrate the main effect of process parameters [23]

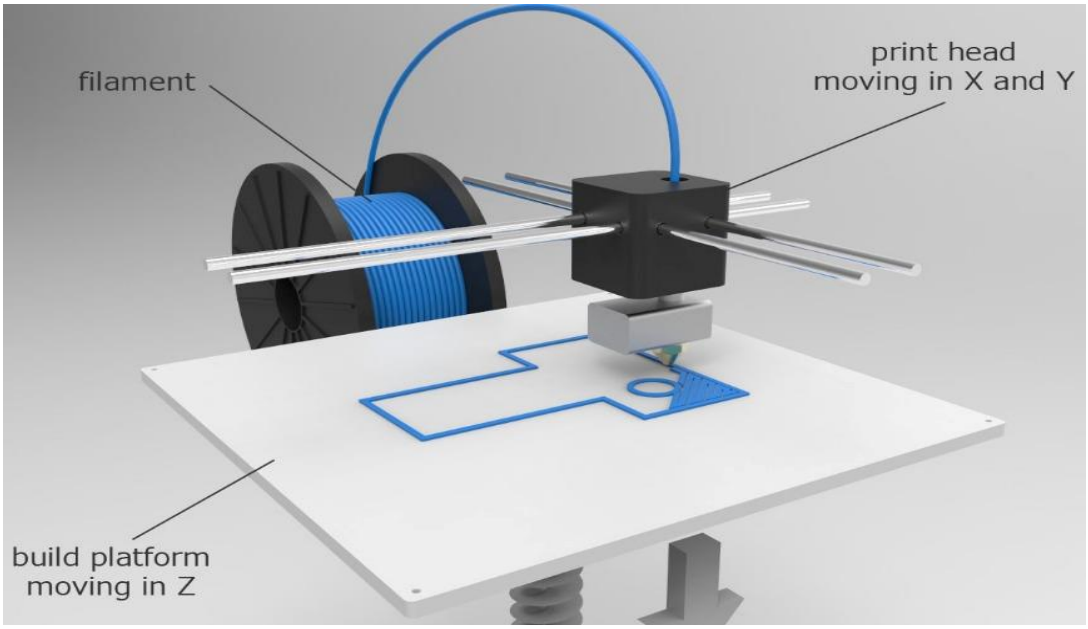

Fig. 2. FDM 3D Printing: Instruction to Fused Deposition Modelling AKA FFF [24]

1.3 Applications:

Aerospace- These companies were some of the first to adopt additive manufacturing. Some of the toughest industry performance standards exist in this realm, requiring parts to hold up in harsh conditions. Engineers designing and manufacturing for commercial and military aerospace platforms need flight-worthy components made from high-performance materials.

With ITAR registration and both ISO 9001 and AS9100 certifications, Stratasys Direct Manufacturing has had the opportunity to see a range of innovative designs transform the production of aerospace parts for major companies. Common applications include environmental control systems (ECS) ducting, custom cosmetic aircraft interior components, rocket engines components, combustor liners, tooling for composites, oil and fuel tanks and UAV components. 3D printing delivers complex, consolidated parts with high strength. Less material and consolidated designs result in overall weight reduction – one of the most important factors in manufacturing for aerospace. Some of the 3D printed spare parts for manufacturing is shown in Fig. 3. The benefits of additive manufacturing for major companies and organizations continues to push forward the innovative designs and applications for the world of flight.

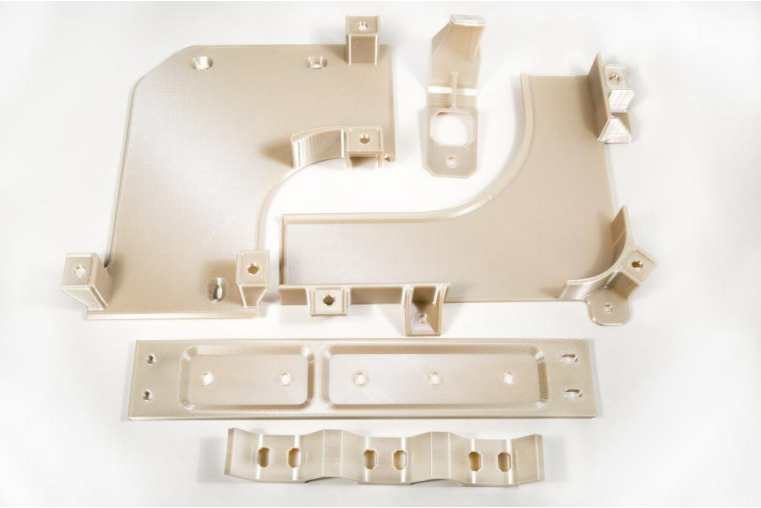

Fig. 3. Added 3D printing for Airbus - Aerospace Manufacturing [25]

Medical - The rapidly innovating medical industry is utilizing additive manufacturing solutions to deliver breakthroughs to doctors, patients and research institutions. Medical manufacturers are utilizing the wide range of high-strength and biocompatible 3D printing materials, from rigid to flexible and opaque to transparent, to customize designs like never before.

From functional prototypes and true-to-life anatomical models to surgical grade components, additive manufacturing is opening the door to unforeseen advancements for life-saving devices. Some applications shaking up the medical industry are orthopedic implant devices, dental devices, pre-surgery models from CT scans, custom saw and drill guides, enclosures etc. and these are also shown in Fig. 4.

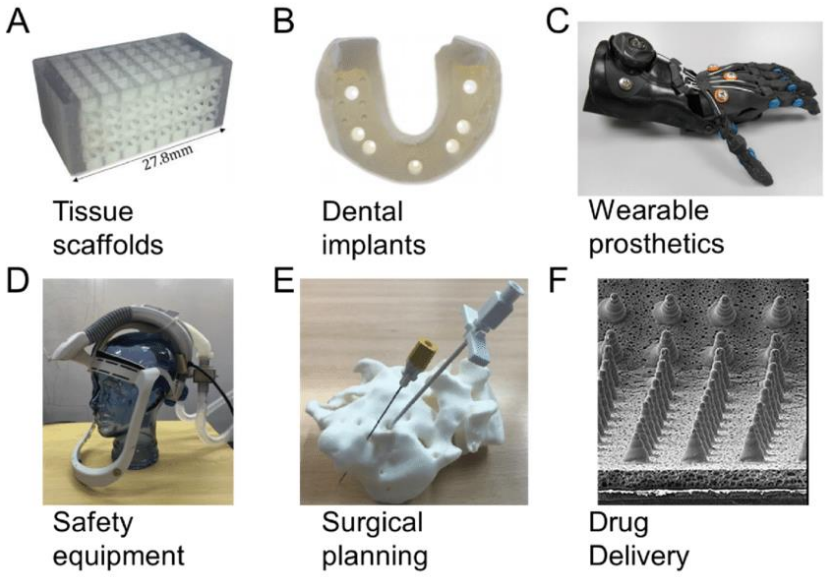

Fig. 4. Medical 3D printing applications for (A) spinal fusion cage, (B) dental model, (C) prosthetic hand , (D) protection equipment , (E) sacral surgery planning, and (F) drug-delivering microneedles [26].

Military- Additive manufacturing, or 3D printing, has become a transformative force in military applications. Its rapid prototyping capabilities allow for swift development of prototypes, customized equipment, and spare parts tailored to specific military needs. This technology significantly reduces supply chain dependencies, enabling on-demand production of components near the battlefield, thereby enhancing operational flexibility and resilience. The ability to create complex geometries, optimize structures for weight reduction, and contribute to the development of stealth technologies makes additive manufacturing a crucial tool in advancing military capabilities. From producing unmanned aerial vehicles (UAVs) to facilitating field repairs and medical applications, 3D printing empowers the military with a versatile and efficient means of manufacturing, ultimately increasing agility and reducing logistical challenges. Example of artificial prosthetic limb hand is shown in Fig. 5.

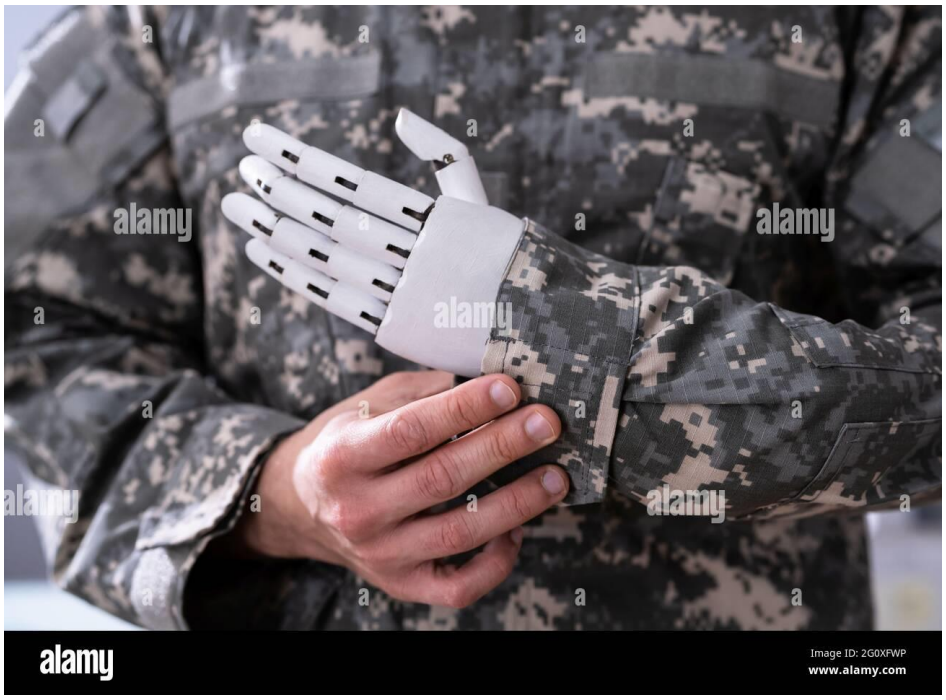

Fig. 5. Soldier Artificial Prosthetic Limb Hand. War Veteran Stock Photo – Alamy [27]

1.4 Machine Learning:

Machine learning is a subset of artificial intelligence (AI) that enables systems to learn from data and make predictions or decisions without being explicitly programmed. It encompasses a variety of algorithms and techniques that allow computers to recognize patterns, extract insights, and adapt their behavior based on experience.

How machine learning can help optimize processes?

- Pattern Recognition: Machine learning algorithms can analyze large datasets to identify patterns and trends that might not be obvious to human analysts. This can help in understanding complex relationships within a process and identifying factors that influence outcomes.
- Predictive Modeling: By analyzing historical data, machine learning models can make predictions about future outcomes. In the context of process optimization, these predictions can be used to anticipate potential issues or opportunities and take proactive measures to improve efficiency or quality.
- Machine learning algorithms can be used to optimize process parameters by iteratively adjusting inputs to achieve desired outputs. This optimization process can be automated and accelerated, leading to more efficient resource utilization and better overall performance.
- Machine learning algorithms can detect unusual or anomalous behavior in a process, which may indicate inefficiencies, errors, or potential failures. By identifying and addressing these anomalies early, processes can be made more robust and reliable.

1.5 Objectives:

- To experimentally study the effects of Extruder Temperature, number of contours, and Layer Thickness on tensile strength of FDM part.
- To build predictive model for estimating the tensile strength of FDM parts using ML models.
- To compare the trustworthiness of the ML models such as SVM and ANN using statistical analysis.

CHAPTER 2: LITERARTURE REVIEW

Additive Manufacturing (AM), also known as 3D printing, has emerged as a transformative technology in recent decades, revolutionizing various industries such as communications, imaging, architecture, and engineering. Unlike traditional manufacturing methods that often involve subtractive processes, where material is removed to shape an object, AM builds objects layer by layer using computer-aided design (CAD) software or 3D object scanners. This digital flexibility and efficiency have paved the way for novel approaches in manufacturing operations.

In the realm of AM, materials like acrylonitrile butadiene styrene (ABS) and polylactic acid (PLA) are widely used, offering unique properties and applications. However, achieving desired mechanical properties and surface finishes in printed parts requires careful consideration of various process parameters. Research indicates that parameters such as nozzle diameter, extrusion temperature, layer thickness, and infill density significantly impact the properties of printed parts. Research indicates that CAD-generated parts tend to have better surface quality compared to manually crafted ones. Among infill patterns, grid and concentric patterns consistently yield the best surface quality, while the zigzag pattern performs the poorest due to its non-optimal design and poor adhesion.

These findings underscore the importance of selecting appropriate infill patterns to achieve desired surface finishes in PLA-printed parts (Jayanth et al., (2018)). Materials like acrylonitrile–butadiene–styrene (ABS) and polylactic acid (PLA) are widely used. Research indicates that varying parameters such as nozzle diameter, liquefier temperature, extrusion velocity, filling velocity, and layer thickness significantly impact the properties of printed parts. Studies show that increasing nozzle diameter, utilizing higher extrusion and filling velocities, and employing thicker layers lead to a substantial increase in tensile strength. Among these parameters, nozzle diameter and layer thickness emerge as the most influential factors affecting tensile strength, surface roughness, and build time (Yang et al., (2019)).

In the context of ABS 3D printing, various parameters such as infill percentage, layer thickness, print speed, and extrusion temperature play crucial roles in determining the mechanical properties of printed parts. Research highlights that the infill percentage primarily influences tensile strength and flexural strength, with higher infill percentages generally resulting in stronger parts. Conversely, extrusion temperature exhibits a significant impact on impact strength, indicating that adjusting this parameter can enhance a part's resistance to sudden forces. Optimal values for tensile strength, impact strength, and flexural strength are determined using approaches such as desirability analysis and nonlinear regression.

These optimized parameters are validated through experimental testing, ensuring the reliability and effectiveness of the chosen settings for achieving desired mechanical properties in ABS-printed parts (Vijayakumar et al., (2022)). (Chadge et al. (2021)) have argued that the tensile strength of PLA parts reaches its maximum at a zero-degree build orientation angle and decreases as the build orientation angle increases. Furthermore, they

observed that surface roughness increases as the building orientation angle is increased from zero degrees to 90° . The study on PLA printing parameters conducted by (Dave et al. (2021)) reveals that tensile strength is impacted similarly by extrusion temperature and infill density. However, extrusion temperature has a more significant influence on tensile strength compared to infill density. The findings suggest that higher extrusion temperatures contribute to increased tensile strength up to a certain threshold.

Atakok, Kam, and Koc, (2021) conducted tests on PLA printing parameters, including layer thickness and infill density. Through statistical analysis, they identified optimal process parameters as 0.25 mm layer thickness, 70% infill density, and PLA filament type. Their findings revealed that layer thickness was the most influential parameter in enhancing mechanical properties. Additionally, a decreasing trend in strength was observed as the infill density decreased. (Vijayaraghavan et al., (2014)) introduced an enhanced method employing MGGP for evaluating wear strength in FDM-produced components. Their proposed model exhibited superior performance compared to standardized MGGP and SVR models and performed comparably to the ANN model. Furthermore, their research revealed that wear strength diminishes with rising layer thickness and raster width, while it increases with increasing air gap.

Garg et al., (2014) compared M5'-GP, SVR, and ANFIS methodologies concerning layer thickness, orientation, raster angle, raster width, and air gap. They found that the M5'-GP method outperformed SVR and ANFIS. Their M5'-GP model, which included layer thickness, orientation, and air gap as input parameters, indicated that these factors significantly influenced compressive strength. In conclusion, the literature review highlights the significant impact of additive manufacturing (AM) processes on various industries, including communications, imaging, architecture, and engineering. The transformative nature of AM lies in its ability to build objects layer by layer using computer-aided design (CAD) software or 3D object scanners, offering unparalleled flexibility and efficiency compared to traditional subtractive manufacturing methods.

Throughout the review, the importance of selecting appropriate process parameters in AM, such as nozzle diameter, extrusion temperature, layer thickness, and infill density, has been underscored. Research indicates that these parameters significantly influence the mechanical properties and surface finishes of printed parts. For instance, studies have shown that CAD-generated parts tend to exhibit better surface quality compared to manually crafted ones, with specific infill patterns, such as grid and concentric patterns, yielding superior results. Furthermore, investigations into materials commonly used in AM, such as acrylonitrile–butadiene–styrene (ABS) and polylactic acid (PLA), have revealed the critical role of process parameters in determining mechanical properties.

Optimal values for parameters such as infill percentage, print speed, and extrusion temperature have been identified using approaches such as desirability analysis and nonlinear regression, ensuring the reliability and effectiveness of the chosen settings for achieving desired mechanical properties. Moreover, recent studies have explored advanced methodologies for evaluating the performance of AM-produced components, such as MGGP, SVR, and ANFIS. These methodologies have provided valuable insights into factors

influencing wear strength and compressive strength, contributing to the ongoing advancement of additive manufacturing technologies. In conclusion, the literature reviewed demonstrates the significant progress made in understanding and optimizing AM processes to enhance part quality and performance. By leveraging the insights gained from these studies, future research and development efforts can continue to drive innovation and efficiency in additive manufacturing, further expanding its applications across various industries.

CHAPTER 3: MATERIALS AND METHODOLOGY

3.1 3D Printer:

This is the printer present in our Material Science Lab as shown in Fig. 6. We printed 13x3 samples of above parameters of dog bone shape as per ASTM D638 standard.

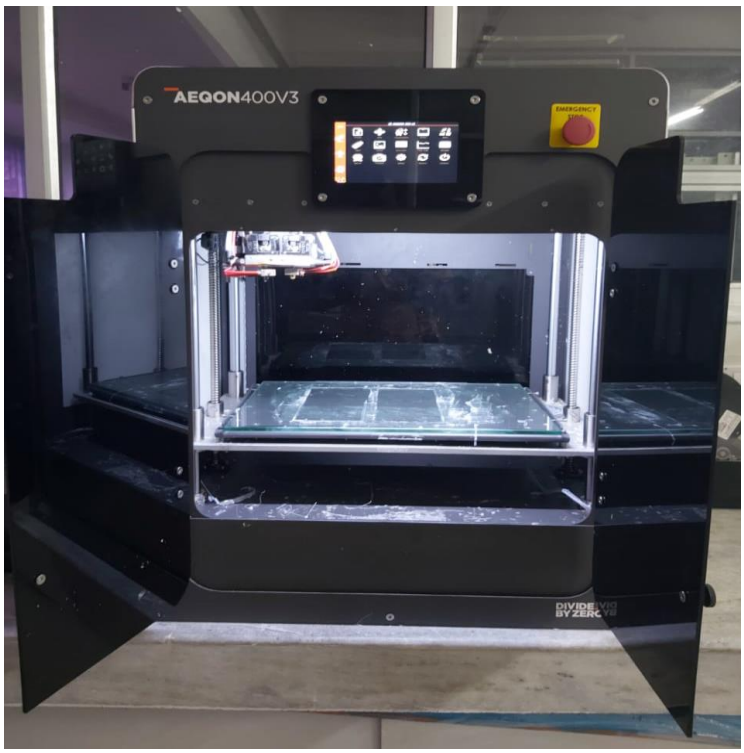

Fig. 6. 3D Printer available in Material Science Lab

We did research on 3D printer and talked to the research scholars about the input parameters and the ranges that we can change in our material science lab.

1) Extrusion Temperature: Extrusion temperature is the temperature the extruder heats to during your print. It depends on a few other variables, mainly the properties of the plastic filament and your print speed.
   Range For PLA: 200 °C to 240 °C
   Range For ABS: 210 °C to 260 °C

2) Layer Thickness: Layer thickness in 3D printing is a measure of the layer height of each successive addition of material in the additive manufacturing or 3D printing process in which layers are stacked.
   Range: 0.1 mm to Nozzle diameter
   Nozzle diameter: 0.4 mm and 0.6 mm

3) Speed: 3D printing speed is contingent upon the height of the material manufactured (or the height of the layers constructed) in a given period.
Speed: 0 to 100%

4) Raster Angle: Raster angle is the angle of the raster tool path deposited with respect to the x-axis of the build table.
Range: 0° to 90°

5) Infill Density: Infill density is that the "fullness" of the within of part. In slicers, this can be usually defined as a percentage between 0 and 100, with 0% making a component hollow and 100% completely solid.
Range: 0 to 100

6) No of Contours/Loops: Each layer of an object is typically composed of one or more perimeters (loops) that define the outer boundaries of that layer. The number of contours or perimeters affects the strength, surface finish, and overall quality of the print. Increasing the number of contours can enhance the structural integrity of the object, but it also increases the printing.
Range: 1 to 5

But after our study we found that there are only few input parameters which affect “Tensile Strength” of 3d printed sample, hence we will vary only 3 parameters- Extrusion Temperature, Layer Thickness and No of Loops/Contours.

3.2 Materials and Properties:

3.2.1 Acrylonitrile Butadiene Styrene (ABS):

ABS stands for Acrylonitrile Butadiene Styrene. It is an impact-resistant engineering thermoplastic. It has an amorphous polymer. ABS is made up of three monomers: acrylonitrile, butadiene, and styrene. Molecular structure has also been given in Fig. 7 and physical properties are given in Table 1.

- Acrylonitrile: It is a synthetic monomer. It is produced from propylene and ammonia. This component contributes to the chemical resistance & heat stability of ABS.
- Butadiene: It is produced as a by-product of ethylene production from steam crackers. This component delivers toughness & impact strength to ABS polymer.
- Styrene: It is manufactured by dehydrogenation of ethyl benzene. It provides rigidity & processability to ABS plastic.

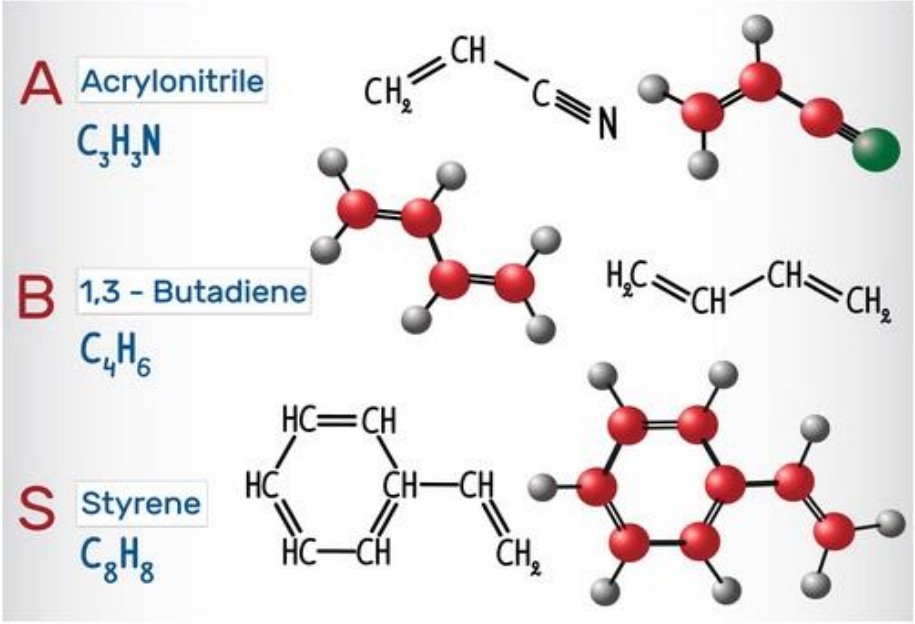

Fig. 7. Molecular Structure of ABS [28]

Chemical Properties of ABS

- Very good resistance to diluted acid and alkalis
- Moderate resistance to aliphatic hydrocarbons
- Poor resistance to aromatic hydrocarbons, halogenated hydrocarbons and alcohols

We used this filament form for our 3D printing which is shown in Fig. 8.

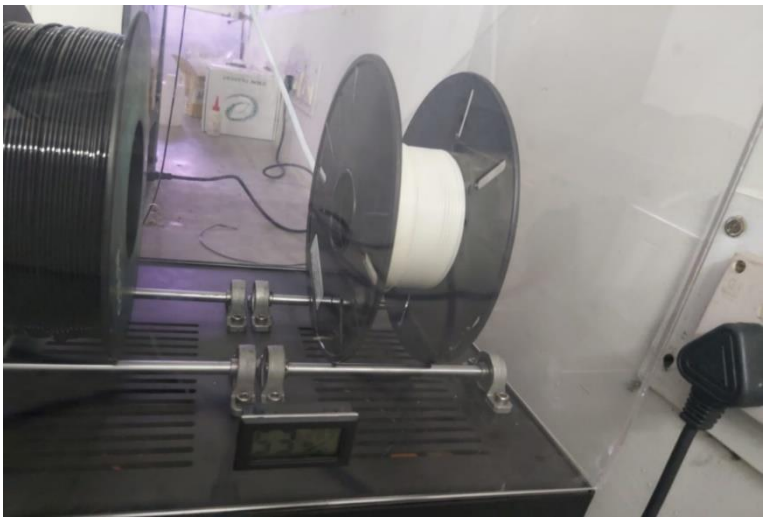
Fig. 8. ABS Filament available in Material Science Lab

Table 1. Mechanical Properties of ABS

Elongation at Break	10 - 50 %
Elongation at Yield	1.7 - 6 %

Flexibility (Flexural Modulus)	1.6 - 2.4 GPa
Hardness Shore D	100
Stiffness (Flexural Modulus)	1.6 - 2.4 GPa
Strength at Break (Tensile)	29.8 - 43 MPa
Strength at Yield (Tensile)	29.6 - 48 MPa
Toughness (Notched Izod Impact at Room Temperature)	200 - 215 J/m
Toughness at Low Temperature (Notched Izod Impact at Low Temperature)	20 - 160 J/m
Young Modulus	1.79 - 3.2 GPa

What are the limitations of ABS?

- Poor weathering resistance
- Ordinary grades burn easily and continue to burn once the flame is removed
- Scratches easily
- Poor solvent resistance, particularly aromatic, ketones and esters
- Can suffer from stress cracking in the presence of some greases
- Low dielectric strength
- Low continuous service temperature

3.2.2 Printing of samples:

The process of printing with a 3D printer typically involved the following steps:

1. Designing: We created or obtained a digital 3D model using computer-aided design (CAD) software. The samples we printed was dog bone shape sample (ASTM D638) shown in Fig. 9.

2. Slicing: The 3D model was sliced into thin horizontal layers using slicing software, which generated instructions (G-code) for the printer. We used KISSSlicer for this step.

3. Preparing: We loaded the ABS filament into the printer's extruder or reservoir. We also leveled the print bed to ensure proper adhesion of the first layer.

4. Printing: The printer's nozzle or print head moved along the X, Y, and Z axes, depositing or

solidifying material layer by layer according to the G-code instructions.

5. Cooling and Finishing: Once printing was complete, we allowed the printed object to cool down before removing it from the print bed. Depending on the material and printer used, we may have applied additional post-processing steps such as sanding, painting, or curing to achieve the desired finish or mechanical properties. After removing from bed we got samples as shown in Fig. 10.

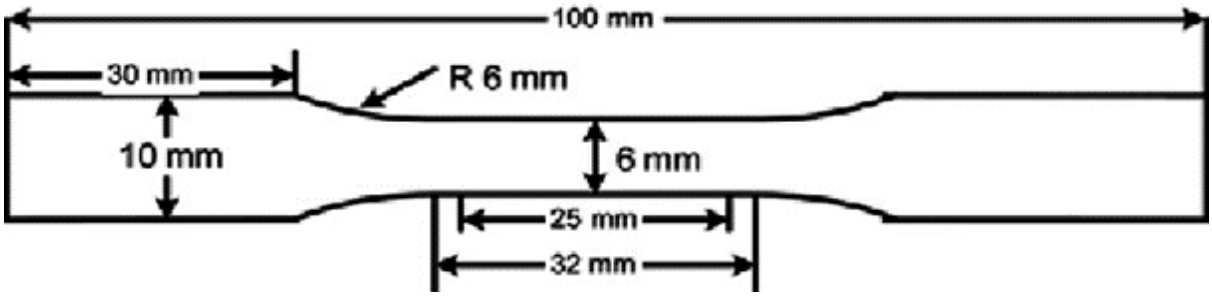

Fig. 9. Dimensions of Dog Bone Samples ASTM D6

Fig. 10. 3D Printed Samples

3.3 Design of Expert (DOE):

Design of Expert (DOE) is a systematic and structured approach to planning, conducting, and analyzing experiments or tests. The goal of DOE is to optimize processes, improve product

quality, and gain a better understanding of the factors that influence a particular outcome. Here's a breakdown of how Design of Experiments works:

1. Define Objectives:
   Clearly define the objectives of the experiment. Determine what you want to achieve or optimize.

2. Identify Factors and Levels:
   Identify the independent variables, often called factors, that may influence the outcome. Determine the different levels of these factors that will be tested.

3. Select Experimental Design:
   Full Factorial Design: Tests all possible combinations of factor levels.
   Fractional Factorial Design: Tests a fraction of the full set of combinations, useful for large experiments.
   Response Surface Design: Explores the relationship between factors and responses in more detail.

4. Randomization:
   Randomly assign experimental units (such as test subjects or samples) to different treatment groups. This helps to minimize the impact of extraneous variables.

5. Replication:
   Replicate each combination of factor levels to ensure the reliability and robustness of the results. Replication helps account for variability.

We got permutation of data from DOE as given in Table 2.

3.4 Tensile Testing:

Apparatus: The Universal Testing Machine (UTM) is a machine with which several tests can be performed, namely, Tension, Compression, Bending, Buckling and Hardness. The movement is controlled by rate of pumping of fluid into a hydraulic cylinder whose piston controls the movement of the moving plate. The load ranges available on the machine are 0-8 ton and 8-20 ton with resolution of 2 kgf and 5 kgf respectively. The ram must be right down before the capacity is changed or the motor is switched off. UTM machine available in our lab is shown in Fig. 11.

Table 2. Permutations generated by DOE

Set_ID	Temperature	Layer Thickness	No. of loops
1	250	0.1	3
2	230	0.25	3
3	210	0.1	3
4	230	0.1	1
5	230	0.4	5
6	250	0.25	5
7	250	0.25	1
8	250	0.4	3
9	210	0.25	1
10	210	0.4	3
11	210	0.25	5
12	230	0.1	5
13	230	0.4	1

Fig. 11. UTM Testing Machine in Strength of Materials Lab

- Model :8801J4051(8800MTB11872)
- Make: INSTRON, UK
- Name: Instron Closed Loop Servo Hydraulic Dynamic Testing Machine
- Capacity: 100 kN
- Maximum travel: 150 mm +/- 5mm
- Tests: tensile, compression, cyclic fatigue, fracture toughness, shear and bend.
- Load cells: 100 kN, 25 kN
- Extensometers: Linear and bi-axial, high temperature
- Control modes: load rate, elongation rate, load hold, strain rate
- Wave forms: Sinusoidal, square, triangular, user specified
- Others: Real time data recording, real time graphs.

An electronic clip-on type extensometer with gauge length 25mm and 50mm is used to indicate the extension between the end points of the gauge length of the specimen to which it is attached. It must be very carefully and should be used only for yield / proof studies and not for specimen failure or breakage (i.e., it must be removed immediately after yield point to avoid damage to the extensometer).

The specimen has a larger diameter at the ends with a smooth fillet connecting to the reduced diameter of the central portion to ensure that the effect of the holding jaws is not significant on the state of stress within the gauge length. The diameter at the middle of the gauge length is reduced by about 20mm to ensure that neck forms in this region so that a meaningful value of percentage elongation is obtained.

The machine frame consists of two cross-heads and lower table. The lower cross-head is adjustable by means of geared motor. Tension test is carried out between lower and upper cross-head. Sensing of the load is done by means of precision pressure transducer of strain gauge type.

The loading unit consists of a robust base. The main hydraulic cylinder is fitted in the centre of the base and piston slides in the cylinder. The lower table is connected to the main piston. This lower table is rigidly connected to the upper cross-head by two straight columns. The chain and sprocket driven by a motor fitted in the base rotates the two straight columns mounted on the base which enables movement of the lower cross-head. The jaws inserted for tensile test specimen along with the rack jaws slide in the lower and 2 upper cross-heads. Jaw locking

handle is provided to lock the jaws of the lower crosshead after the specimen is clamped. An elongation scale is kept sliding on the rod which is fixed between the lower table and upper crosshead. The elongation indicating pointer is fixed to the lower cross-head.

The control panel has two control valves to control oil flow in the hydraulic system, one at the right side and the other at the left. The right-side valve is a pressure compensated flow control valve. The left side valve is a return valve, i.e., it allows the oil from the cylinder to go back to the tank. Pressure compensation of the flow control keeps a constant rate of straining regardless of the total load on the specimen.

PROCEDURE: Before testing, adjust the load range according to the capacity of the test piece. Measure the diameter of the specimen. Mark the gauge length of the specimen. Select the proper jaw inserts and complete the upper and lower chuck assemblies. Then operate the upper cross-head grip operation handle and grip fully the upper end of the test piece. Attach the extensometer to the specimen. Apply the load gradually and read the extension from the extensometer at equal increments of load till yield occurs. Remove the extensometer. Increase the displacement of the movable jaw till the specimen fractures in into two pieces. Note down the maximum load applied. Measure the minimum diameter of the necked section and final deformed lengths between the marked gauge points by assembling together the fractured pieces.

LOADING / UNLOADING: The left valve is kept in fully closed position and the right valve in normal open position. Open the right valve and close it after the lower table is slightly lifted. Now adjust the load to zero by Tare push button. (This is necessary to remove the dead weight of the lower table, upper cross-head and connecting parts from the load). Operate the lower grip operation handle and lift the lower cross-head up and grip fully the lower part of the specimen. Then lock the jaws in this position by operating the jaw locking handle then turn the right control valve solely to open position, (i.e., anticlockwise) until you get a desired loading rate. After this you will find that the specimen is under load and then unclasp the locking handle. Now the jaws will not slide down due to their own weight. Then go on increasing the load when the test piece is broken. Then open the left control valve to take the piston down.

After conducting the tensile tests on the samples and recording all observations, the tensile strength of all 13 combinations was documented in Table 3. Each combination is represented by a unique SET_ID, indicating a permutation of input parameters.

Subsequently, we created a graph plotting the tensile strength against the SET_ID. This plot, displayed in Fig.12, visually represents the relationship between the input parameter combinations and the resulting tensile strengths.

Table 3. UTS Result

Set ID	Temperature (C)	Layer Thickness(mm)	No. of loops	Tensile Stress (MPa)
1	250	0.1	3	39.02920
2	230	0.25	3	39.24605
3	210	0.1	3	42.17957
4	230	0.1	1	38.51772
5	230	0.4	5	36.15715
6	250	0.25	5	37.80847
7	250	0.25	1	37.37158
8	250	0.4	3	36.14215
9	210	0.25	1	34.92265
10	210	0.4	3	36.42809
11	210	0.25	5	41.77883
12	230	0.1	5	41.38440
13	230	0.4	1	31.73968

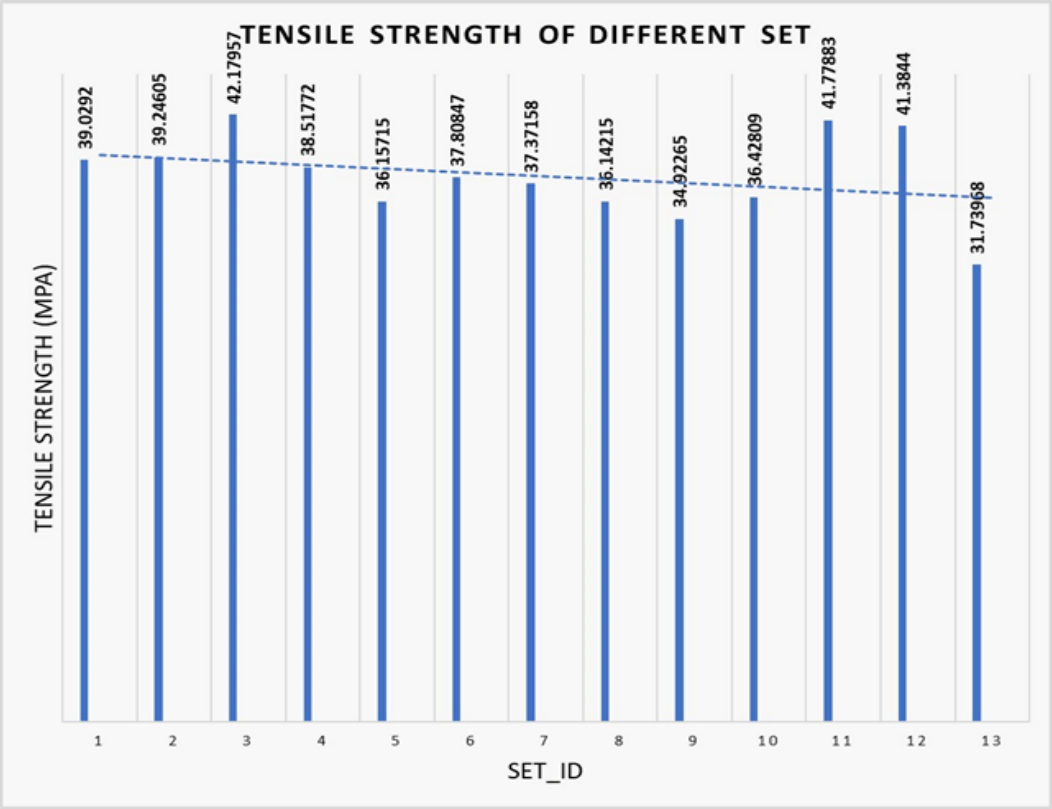

Fig. 12. Histogram image of Tensile Strength vs different SET__ID

3.5 Machine Learning Models:

3.5.1 Artificial Neural Network (ANN):

Artificial Neural Networks (ANNs) are computational models inspired by the human brain's biological structure. A neuron cell in Human brain is shown in Fig, 13. They consist of interconnected artificial neurons that process information. ANNs utilize connection weights to store information and can process extensive data, making predictions with surprising accuracy. However, their capabilities do not equate to human-like intelligence.

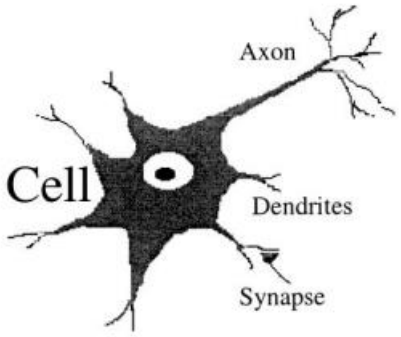

Fig. 13. Neuron Cell [29]

The artificial neuron, the basic unit of an ANN, receives inputs, multiplies them by connection weights, aggregates them, and passes them through an activation function to produce an output. Connectivity patterns in ANNs, including excitatory and inhibitory inputs, lateral inhibition, and feedback connections, significantly influence network behavior. Model of an artificial neuron is shown in Fig. 14.

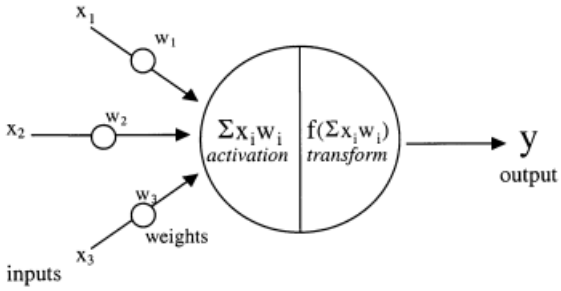

Fig. 14. Model of an artificial neuron [29]

Learning in ANNs involves adjusting connection weights to minimize prediction errors. The most common learning rule is the Delta rule or Back-propagation rule, which iteratively optimizes weights through backward propagation of errors. Training aims to achieve a specified level of accuracy while avoiding overfitting, where the network becomes overly specialized to training data.

Structure of ANN:

1. Input Layer:
    - $X=[x1,x2,...,xn]$ represents the input features.
    - n is the number of input features.
    - xi represents the i-th input feature.
2. Hidden Layers:
    - Each hidden layer consists of neurons that perform computations on the input data.
    - The output of each neuron in a hidden layer is computed as follows:

$$z_j^{(l)} = \sum_{i=1}^{n^{(l-1)}} w_{ij}^{(l)} \cdot a_i^{(l-1)} + b_j^{(l)}$$
$$a_j^{(l)} = f(z_j^{(l)})$$

$z_j^{(l)}$ is the weighted sum of inputs to neuron j in layer l.

    - $wij(l)$ is the weight connecting neuron i in layer $l-1$ to neuron j in layer l.
    - $ai(l-1)$ is the activation of neuron ii in layer $l-1$.
    - $bj(l)$ is the bias term for neuron j in layer l.
    - $f(\cdot)$ is the activation function applied element-wise to the weighted sum.
3. Output Layer:
    - The output layer produces the final predictions or classifications.
    - The output of the network is computed as the activation of neurons in the output layer: $\hat{y} = a_1^{(L)}$
    - LL is the index of the output layer.
    - $y^$ represents the predicted output.

Functioning of ANN:

1. Forward Propagation: During forward propagation, input data is passed through the network layer by layer. Each neuron in a layer receives inputs from the neurons in the previous layer, computes a weighted sum of these inputs, applies an activation function to the sum, and passes the result to the neurons in the next layer. Feed Forward network is shown in Fig. 15.

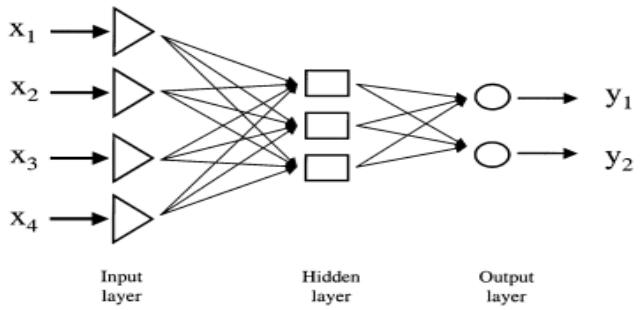

Fig. 15. Feedforward network [29]

2. Activation Functions: Activation functions introduce non-linearity to the network, enabling it to learn complex patterns in the data. Common activation functions include sigmoid, tanh, ReLU (Rectified Linear Unit), and softmax.

   Common activation functions used in ANNs include:

   1. Sigmoid Function (Logistic):

$$\sigma(x) \doteq \frac{1}{1+e^{-x}}$$

   2. Hyperbolic Tangent (tanh) Function:

$$\tanh(x) \doteq \frac{e^{x}-e^{-x}}{e^{x}+e^{-x}}$$

   3. Rectified Linear Unit (ReLU):

$$\begin{aligned}(x)^{+} &\doteq \begin{cases} 0 & \text{if } x \leq 0 \\ x & \text{if } x > 0 \end{cases} \\ &= \max(0,x) = x\mathbf{1}_{x>0}\end{aligned}$$

3. Training: Training an ANN involves adjusting the weights and biases of the connections between neurons to minimize the difference between the predicted outputs and the actual outputs. This process is typically done using optimization algorithms like gradient descent and backpropagation. Supervised network with backpropagation learning rule is shown in Fig. 16.

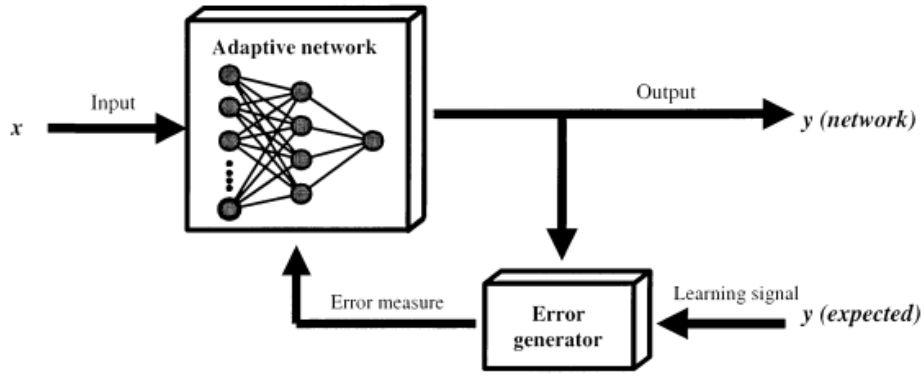

Fig. 16. Supervised network with backpropagation learning rule [29]

4. Backpropagation: Backpropagation is a key algorithm for training ANNs. It calculates the gradient of the loss function with respect to the weights of the network and updates the weights accordingly to minimize the loss. Feedback network is shown in Fig. 17.

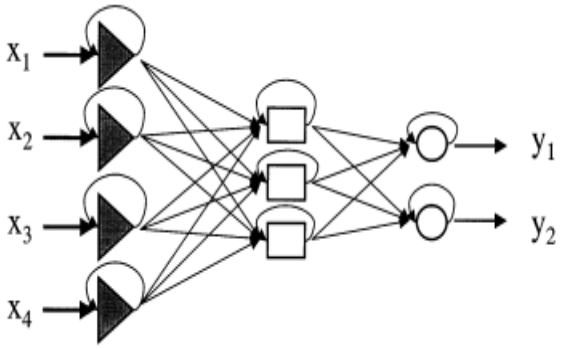

Fig. 17. Feedback network [29]

Applications of ANN:

ANNs have found applications in various domains, including:

- Image Recognition: ANNs are used for tasks such as object detection, image classification, and facial recognition.
- Natural Language Processing (NLP): ANNs are applied to tasks like sentiment analysis, language translation, and text generation.
- Predictive Analytics: ANNs are used for predicting future trends, financial markets, customer behavior, and more.
- Medical Diagnosis: ANNs assist in diagnosing diseases, analyzing medical images, and predicting patient outcomes.
- Robotics and Control Systems: ANNs are employed in autonomous vehicles, robotic arms, and industrial control systems.

Challenges and Considerations:

- Overfitting: ANNs may memorize noise in the training data, leading to poor generalization on unseen data. Regularization techniques such as dropout and weight decay are used to mitigate overfitting.
- Hyperparameter Tuning: ANNs have several hyperparameters (e.g., number of layers, number of neurons, learning rate) that need to be tuned for optimal performance. Techniques like grid search and random search are used for hyperparameter tuning.
    - Number of Layers (num_layers): This hyperparameter defines the number of layers in the neural network architecture, including both hidden layers and the output layer.
    - Number of Neurons per Layer (units_layer_i): For each layer, this hyperparameter determines the number of neurons (also known as units) in that layer. Different layers may have different numbers of neurons, allowing flexibility in model complexity.
    - Learning Rate (learning_rate): The learning rate controls the step size at which the weights of the neural network are updated during the training process. A higher learning rate can lead to faster convergence but may risk overshooting the optimal solution, while a lower learning rate may converge more slowly but with greater stability.
    - Batch Size: Batch size refers to the number of training examples utilized in each iteration of the training process. Larger batch sizes may result in faster training but require more memory, while smaller batch sizes may lead to more noisy updates but better generalization.
    - Epochs: An epoch corresponds to one complete pass through the entire training dataset during the training process. The number of epochs defines how many times the training process iterates over the dataset.
    - Regularization Parameters: Regularization techniques such as L1 and L2 regularization can be employed to prevent overfitting by penalizing large weights in the neural network. The regularization parameter controls the strength of the regularization penalty.
    - Optimizer Algorithm: The optimizer algorithm determines how the weights of the neural network are updated based on the computed gradients during the training process. Popular optimizer algorithms include Adam, SGD (Stochastic Gradient Descent), and RMSprop.
    - The Mean Squared Error (MSE) and $R2$ (R-squared) are commonly used metrics to evaluate the performance of the neural network model:

- Mean Squared Error (MSE): MSE measures the average squared difference between the actual and predicted values of the target variable. It is calculated as the average of the squared residuals:

$$MSE = \frac{1}{n}\sum_{i=1}^{n}(y_i - \hat{y}_i)^2$$

where n is the number of samples, yi is the actual value of the target variable for sample i, and y^i is the predicted value of the target variable for sample i.

- R^2 (R-squared): R^2 measures the proportion of the variance in the dependent variable that is explained by the independent variables in the model. It is calculated as:

$$R^2 = 1 - \frac{SS_{\text{residual}}}{SS_{\text{total}}}$$

where SSresidual is the sum of squares of the residuals (differences between the actual and predicted values), and SStotal is the total sum of squares.

- Tuning hyperparameters and optimizing the model based on these metrics are essential steps in developing an effective neural network model for a given task.

- Computational Complexity: Training large ANNs on complex datasets can be computationally intensive and require high computational resources.
- Interpretability: Understanding the decisions made by ANNs can be challenging due to their black-box nature. Techniques such as feature importance analysis and model visualization are used to interpret ANN decisions.

3.5.2 Support Vector Regression:

SVM is a supervised ML algorithm that can be used for compound classification and ranking and SVR is an extension of SVM that is used for predicting numerical values. SVR stands for Support Vector Regression, a machine learning algorithm used for regression tasks. It's a type of supervised learning algorithm that analyses data and recognizes patterns, then makes predictions based on those patterns. Here's a breakdown of its key aspects:

What is SVR?
Support Vector Regression (SVR) is a type of Support Vector Machine (SVM) algorithm, primarily used for regression (predicting continuous values) rather than classification (predicting discrete labels). Fig. 18 shows a hyperplane classifying input data.

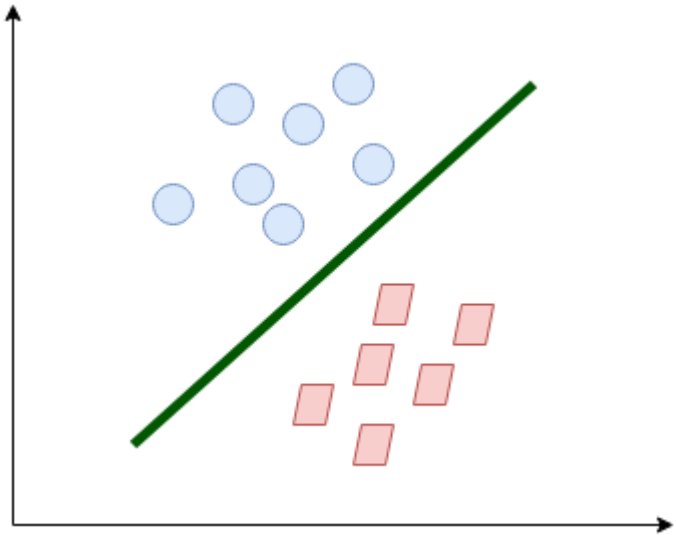

Fig. 18. A hyperplane classifying between two input data [31]

How does SVR work?

1. Data Transformation: SVR works by transforming the input data into a higher dimensional space. This transformation is achieved using a kernel function. Fig. 19 shows how kernel function transforms the input.

2. Identification of Hyperplane: In this transformed space, SVR identifies a hyperplane that best separates the data into different classes. This hyperplane is chosen such that the margin between the hyperplane and the closest data points (called support vectors) is maximized.

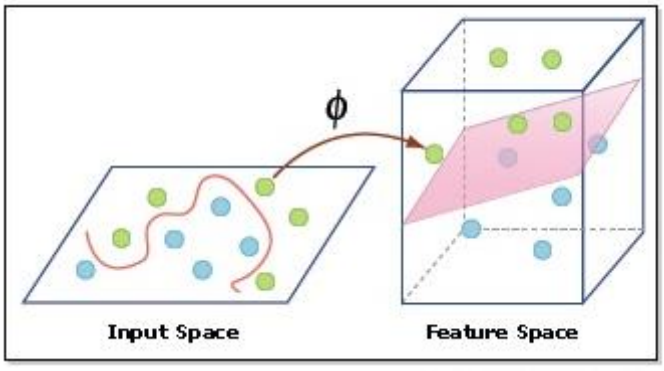

Fig. 19. A kernel function transforms input [31]

3. Regression: SVR aims to fit as many instances as possible within the margin while minimizing the deviation of points from the hyperplane. The goal is to find a function that approximates the mapping from input variables to output variables with minimal error. Fig. 20 shows a SVR using e-sensitive.

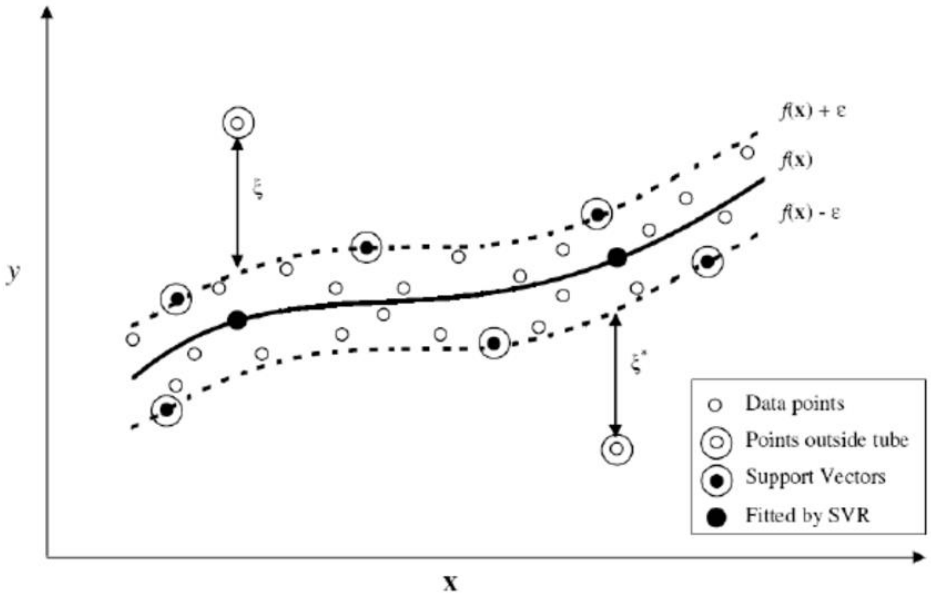

Fig. 20. A schematic diagram of the support vector regression using e-sensitive [32]

Advantages of SVR:

1. Effective in High-Dimensional Spaces: SVR works well even in cases where the number of dimensions exceeds the number of samples.
2. Robust to Overfitting: It is less prone to overfitting compared to other regression algorithms.
3. Flexibility: SVR allows the use of different kernel functions to handle various types of data and relationships.
4. Works with Non-Linear Data: It can effectively model non-linear relationships between input and output variables.

Applications of SVR:

1. Financial Forecasting: SVR can be used to predict stock prices, currency exchange rates, and other financial indicators.
2. Medicine and Healthcare: It's used for predicting disease progression, patient prognosis, and treatment outcomes.
3. Environmental Science: SVR can predict environmental parameters like pollution levels, weather forecasting, and climate change modeling.
4. Engineering and Manufacturing: It's employed in predictive maintenance, quality control, and process optimization in manufacturing industries.
5. Computer Vision: SVR is utilized in image processing tasks such as object recognition, image reconstruction, and medical image analysis.

Functions of SVR:

1. Kernel Functions:

   Kernel functions are fundamental to SVR as they transform the input data into a higher-dimensional space where the data might be linearly separable.

   - Types of Kernel Functions:
     - Linear Kernel: Represents linear transformations and works well for linearly separable data.
     - Polynomial Kernel: Performs polynomial transformations and is suitable for data with polynomial relationships.
     - Radial Basis Function (RBF) Kernel: Utilizes a Gaussian function to map data into an infinite-dimensional space, effective for capturing complex non-linear relationships.
     - Sigmoid Kernel: Maps data into a higher-dimensional space using a sigmoid function.

2. Loss Function:
   - Penalizing Deviations: SVR aims to minimize the deviation of points from the hyperplane while still fitting as many instances within a specified margin.
   - Epsilon-Insensitive Loss: This loss function ignores errors within a certain range (epsilon) and penalizes only larger deviations.
   - Squared Loss: Another common loss function, which penalizes the squared difference between the predicted and actual values.

3. Regularization:
   - Controlling Model Complexity: SVR includes a regularization parameter (C) that balances the trade-off between the margin width and the training error.
   - High C Values: Lead to a narrower margin and may result in overfitting the training data.
   - Low C Values: Lead to a wider margin and may result in underfitting the training data.

4. Decision Function:
   - Determining Predictions: Once the SVR model is trained, it utilizes a decision function to make predictions for new, unseen data points.
   - Calculating Distance to Hyperplane: The decision function calculates the distance of the new data points from the hyperplane and predicts the output based on this distance.

- Using Support Vectors: The decision function mainly relies on the support vectors, which are the data points that lie closest to the hyperplane and determine its position.

5. Parameter Tuning:
    - Optimizing Performance: SVR requires careful parameter tuning to achieve optimal performance.
    - Grid Search or Cross-Validation: Techniques like grid search or cross-validation are often used to find the best combination of parameters, such as the choice of kernel and its parameters, as well as the regularization parameter (C).
6. Training Algorithm:
    - Sequential Minimal Optimization (SMO): This is a popular algorithm for training SVR models. It iteratively optimizes the Lagrange multipliers associated with the support vectors.
    - Working with Large Datasets: SVR algorithms are designed to efficiently handle large datasets, making them suitable for real-world applications with substantial amounts of data.
7. Prediction:
    - Making Predictions: Once trained, an SVR model can be used to predict the output values for new input data points.
    - Scalability: SVR models are scalable and can handle large amounts of data, making them suitable for deployment in production environments.

Limitations:

1. Computationally Intensive: Training SVR models can be computationally expensive, especially with large datasets.
2. Sensitive to Kernel Choice: Performance can heavily depend on the choice of kernel and its parameters.
3. Interpretability: SVR models are not very interpretable, making it challenging to understand the underlying decision-making process.

3.5.3 Data for training and testing:

We used 9 combinations for training and 4 combinations for testing taking validation split as 0.3 from 13 combinations as given in Table 4 and Table 5.

Table 4. Training Data

Set_ID	Temperature	Layer Thickness	No. of loops
1	250	0.1	3
2	230	0.25	3
3	210	0.1	3
4	230	0.1	1
5	230	0.4	5
6	250	0.25	5
7	250	0.25	1
8	250	0.4	3
9	210	0.25	1

Table 5. Testing Data

Set_ID	Temperature	Layer Thickness	No. of loops
1	210	0.4	3
2	210	0.25	5
3	230	0.1	5
4	230	0.4	1

CHAPTER 4: RESULTS AND DISCUSSION

4.1 Model graph analysis of Tensile Strength using DOE:

We have put Tensile Strength data of each permutation in Design of Expert and obtained these model graphs between Tensile Strength and various input parameters.

Varying Extrusion Temp and Layer Thickness keeping No of Outer Loops / Contours =1

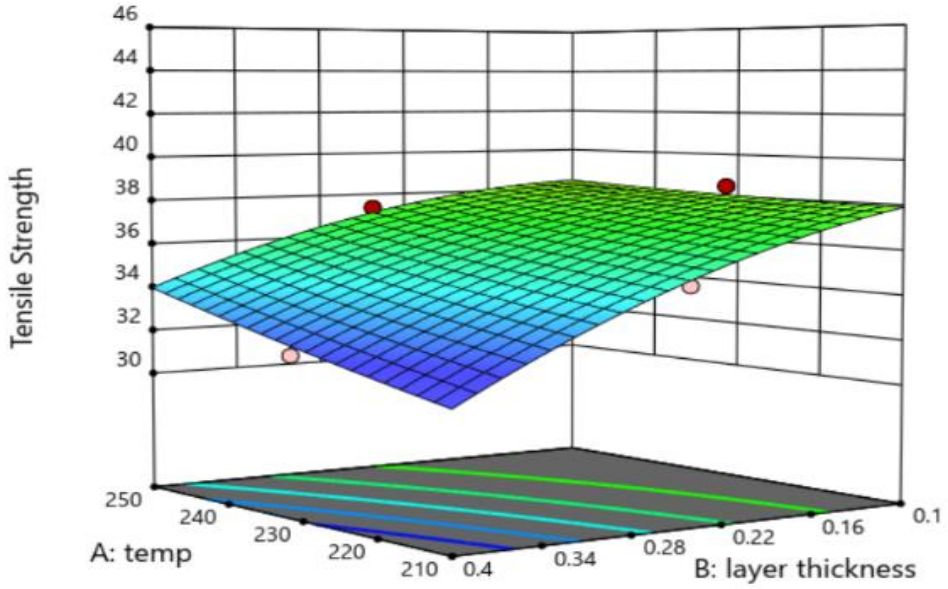

Fig. 21. 3D surface plots for the interactions between Temp and layer thickness for Tensile Strength for No of Outer Loops / Contours =1

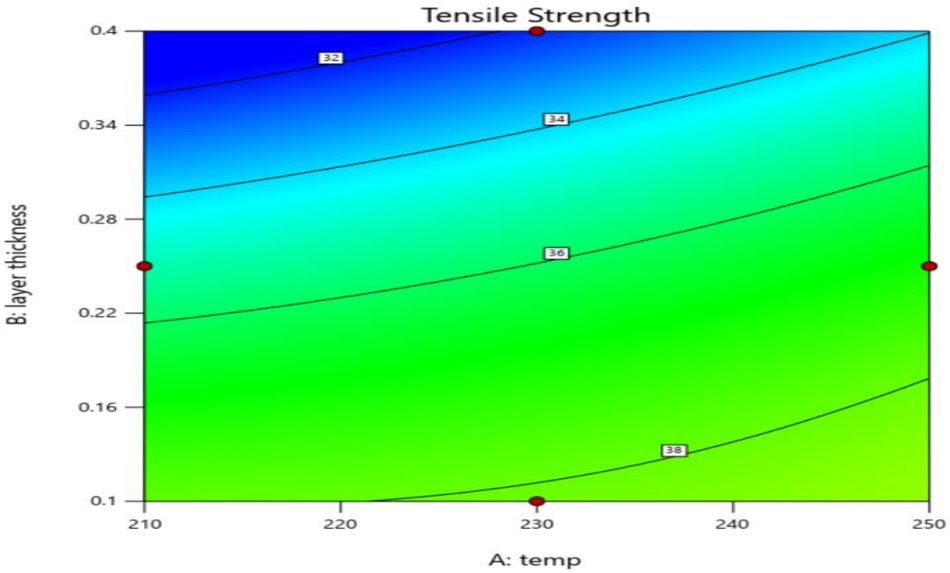

Fig. 22. 2D line plots for the interactions between Temp and layer thickness for Tensile Strength for No of Outer Loops / Contours =1

Varying Extrusion Temp and Layer Thickness keeping No of Outer Loops / Contours =3

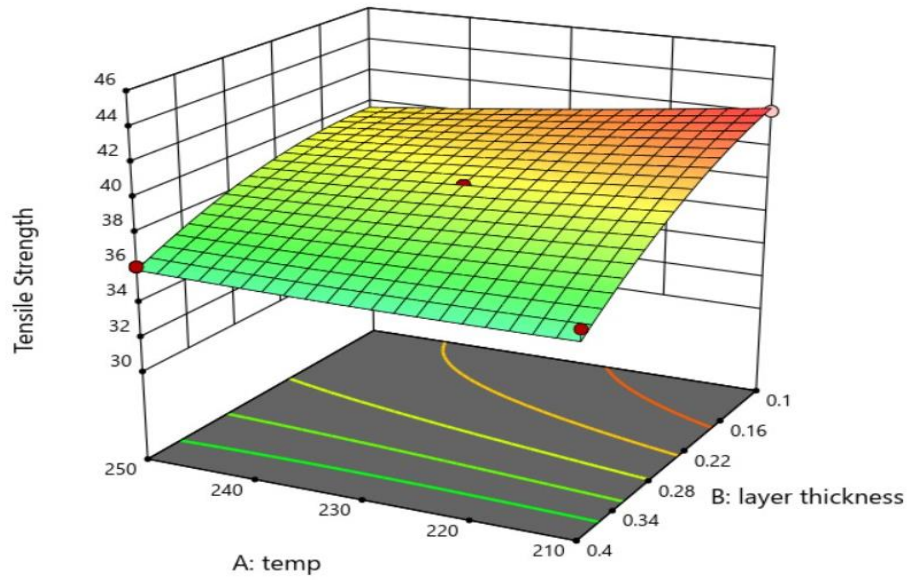

Fig. 23. 3D surface plots for the interactions between Temp and layer thickness for Tensile Strength for No of Outer Loops / Contours =3

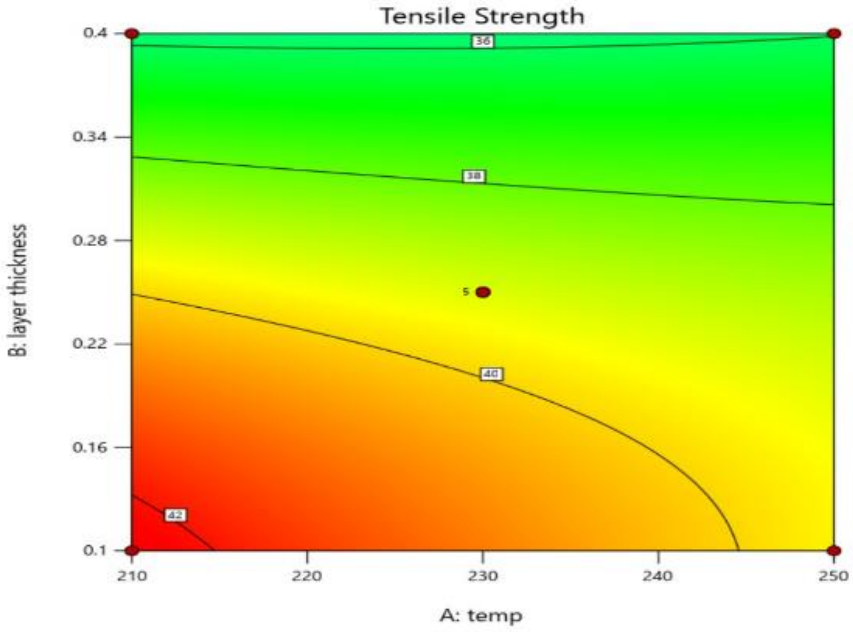

Fig. 24. 2D line plots for the interactions between Temp and layer thickness for Tensile Strength for No of Outer Loops / Contours =3

Varying Extrusion Temp and Layer Thickness keeping No of Outer Loops / Contours =5

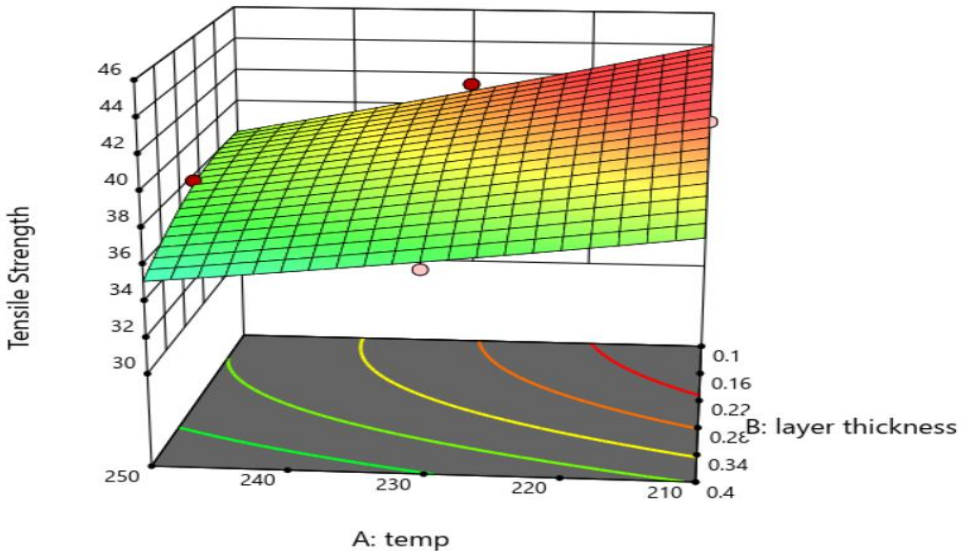

Fig. 25. 3D surface plots for the interactions between Temp and layer thickness for Tensile Strength for No of Outer Loops / Contours =5

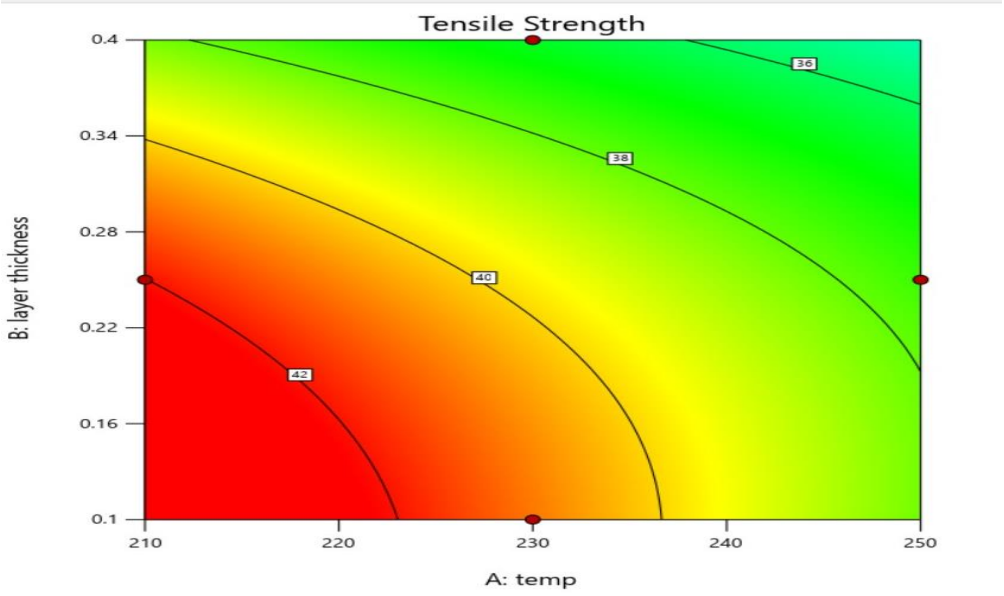

Fig. 26. 2D line plots for the interactions between Temp and layer thickness for Tensile Strength for No of Outer Loops / Contours =5

1. We can see in the Fig. 22 where no of outer loops is equal to 1, on decreasing layer thickness, Tensile Strength is increasing whereas on increasing temp Tensile Strength is increasing.

   But here we can observe one thing that value of Tensile Strength is larger when layer thickness is less compared to when layer thickness is more for same temp.

   Maximum value of Tensile Strength can be found in the area of moderate temp and low layer thickness range. That is equal to 38.51772 MPa on temp=230 C, layer thickness =0.1 and no of contours=1.

2. We can see in the Fig. 24 where no of outer loops is equal to 3, on decreasing layer thickness, Tensile Strength is increasing whereas on increasing temp, Tensile Strength is decreasing.

   But here also we can observe one thing that value of Tensile Strength is varying significantly with temp when layer thickness is less compared to when layer thickness is more. Tensile Strength is almost constant when layer thickness is close to 0.4.

   Maximum value of Tensile Strength can be found in the area of low temp and low layer thickness range. That is equal to 42.17957 MPa on temp=210 C, layer thickness =0.1 and no of contours=3.

3. We can see in the Fig. 26 where no of outer loops is equal to 5, on decreasing layer thickness, Tensile Strength is increasing whereas on increasing temp, Tensile Strength is decreasing.

   But here also we can observe that value of Tensile Strength is varying significantly with temp when layer thickness is less compared to when layer thickness is more. Tensile Strength is more for same temp in low layer thickness range.

   Maximum value of Tensile Strength can be found in the area of low temp and mid layer thickness range. That is equal to 41.77883 MPa on temp=210 C, layer thickness =0.25 and no of contours=5.

4.2 Results from ANN:

This is the best model we got using ANN with mean square error and parameters used is given in Table 6.

Table 6. Parameters Settings for ANN

Parameters	Values Assigned
Training data set	9
Testing data set	4
Number of hidden layers	1-20
Number of neurons in hidden layer	2-1000
Activation	Sigmoid
Number of epochs	1000
Learning rate	0.70
Architecture selection	Trial and error
Target goal mean square error	<10

Code used in training ANN model is given in appendix.

The summary of best model is given in Table 7.

Table 7. Hidden Parameters of model

Value	Hyperparameter
17	Number of layers
98	No of neurons in units_layer_0
0.7	Learning rate
354	No of neurons in units_layer_1
610	No of neurons in units_layer_2
34	No of neurons in units_layer_3
290	No of neurons in units_layer_4
834	No of neurons in units_layer_5
130	No of neurons in units_layer_6
802	No of neurons in units_layer_7
514	No of neurons in units_layer_8
770	No of neurons in units_layer_9
194	No of neurons in units_layer_10
322	No of neurons in units_layer_11
418	No of neurons in units_layer_12
322	No of neurons in units_layer_13

130	No of neurons in units_layer_14
130	No of neurons in units_layer_15
34	No of neurons in units_layer_16
20	tuner/epochs
7	tuner/initial_epoch
1	tuner/bracket
1	tuner/round
0018	tuner/trial_id

Best val_mean_squared_error So Far = 16.8142
R^2 = 0.0038

Interpretation:

- The provided output indicates that the model's architecture and hyperparameters have been optimized based on the training data.
- However, the resulting model's predictive performance, as indicated by the R-squared value, is very low. This suggests that the model's predictions do not accurately capture the variance in the target variable.
- Further analysis and possibly adjustments to the model architecture, hyperparameters, or dataset may be necessary to improve predictive performance.

Overall, while the optimization process has resulted in a neural network configuration with a low validation MSE, the model's ability to accurately predict the target variable remains limited, as indicated by the low R-squared value.

4.3 Results from SVR:

```
param_grid  = [
              'C': [0.1, 1, 10],
              'gamma': ['scale', 'auto'],
              'kernel': ['rbf', 'linear']
             ]
```

We will iterate through every combination of these parameters to get best model with the help of SVR code given in appendix.
We got the Best Parameters given in Table8.
Table 8. Best Parameters of SVR

Parameters	Values Obtained
C	1
gamma	scale
kernel	linear

We got the Mean Squared Error = 7.4765 and
R-squared = 0.65658

Interpretation:

- C Parameter (Regularization parameter): With a value of 1, the SVR model is moderately regularized, meaning it strikes a balance between fitting the training data well and preventing overfitting.
- Gamma Parameter (Kernel coefficient): Using 'scale' as the gamma value, the model adjusts the influence of individual training samples. A 'scale' value means the inverse of the number of features is used to calculate gamma.
- Kernel Function: The choice of 'linear' kernel indicates that the model uses a linear function to map the input variables to the target variable. This suggests that the relationship between the input features and the target variable is assumed to be linear.

Prediction and Influence:

- The SVR model, with the chosen parameters, makes predictions by creating a linear decision boundary between data points in the feature space.
- It weighs each input feature according to their influence on the target variable, with the weights adjusted during training to minimize the prediction errors.
- The 'C' parameter controls the trade-off between achieving a low training error and a low complexity model. A higher 'C' value may result in a narrower margin hyperplane, which may lead to a higher variance but lower bias.
- The 'gamma' parameter, with a value of 'scale', implies that the influence of each training sample is inversely proportional to the number of features. This helps in preventing overfitting by regularizing the model.
- The linear kernel indicates that the model assumes a linear relationship between the input features and the target variable. Therefore, the model's predictions are influenced by linear combinations of the input features.

Overall, the SVR model with the specified parameters demonstrates a reasonable predictive performance, as indicated by the MSE and R-squared values. It provides insights into how the input features influence the target variable and makes predictions based on a linear relationship between them.

4.4 Comparison of Models:

Table 9. Result from SVR and ANN model

Model	MSE	R-squared
SVR	7.4765	0.65658
ANN	16.8142	0.0038

Considering the performance metrics provided for both the SVR and ANN models given in Table 9.
It's evident that the SVR model outperforms the ANN model in both metrics. The SVR has a substantially lower MSE, indicating that it makes more accurate predictions compared to the ANN. Additionally, the SVR exhibits a significantly higher R-squared value, indicating that it explains a larger proportion of the variance in the target variable compared to the ANN.

Based on these results, it would be advisable to choose the Support Vector Regressor (SVR) for this particular dataset, as it demonstrates superior predictive performance and better captures the underlying patterns in the data.

4.5 Sensitivity analysis:

For the validation of the proposed Support Vector Regression (SVR) model, a sensitivity analysis (SA) and parametric analysis were conducted to assess the impact of input parameters on the predicted tensile strength of FDM fabricated components.
The sensitivity analysis determined the percentage of outputs to each input parameter using the following formulas:

$$L_i = f_{\max}(x_i) - f_{\min}(x_i) \qquad \mathrm{SA}_i = \frac{L_i}{\sum_{j=1}^{n} L_j} \times 100$$

where $f\max(xi)$ and $f\min(xi)$ represent the maximum and minimum predicted outputs over the i-th input domain, respectively, while other variables are held constant at their mean values.
Table 10 presents the sensitivity results of input variables in predicting the tensile strength of FDM fabricated components. It indicates that Layer Thickness has the highest impact on tensile strength, followed by Temperature, while the influence of Number of Loops is minimal. This highlights the significance of regulating layer thickness to achieve the greatest variation in tensile strength.

Table 10. Amount of impact of each input variable to the Tensile strength

Input variables	Relative contribution (%) to Tensile strength
Temperature	21.3287
Layer thickness	61.45697
No of Loops	17.21433

The parametric analysis provides insights into the relative importance of model inputs and illustrates how tensile strength varies with changes in input variables. Figure 27 displays plots for each input variable and tensile strength, revealing, for example, a decrease in tensile

strength with increasing layer thickness and an increase with the number of loops. Tensile strength follows a parabolic non-linear relation with the number of loops and layer thickness. Based on the findings from Table 10 and Figure 27, optimal values of input variables can be selected to optimize tensile strength. This enables the proposed model to provide insights into the impact of input process parameters on tensile strength, facilitating informed decision-making in component fabrication processes. Variation of Tensile strength on each parameter is shown in Fig 27.

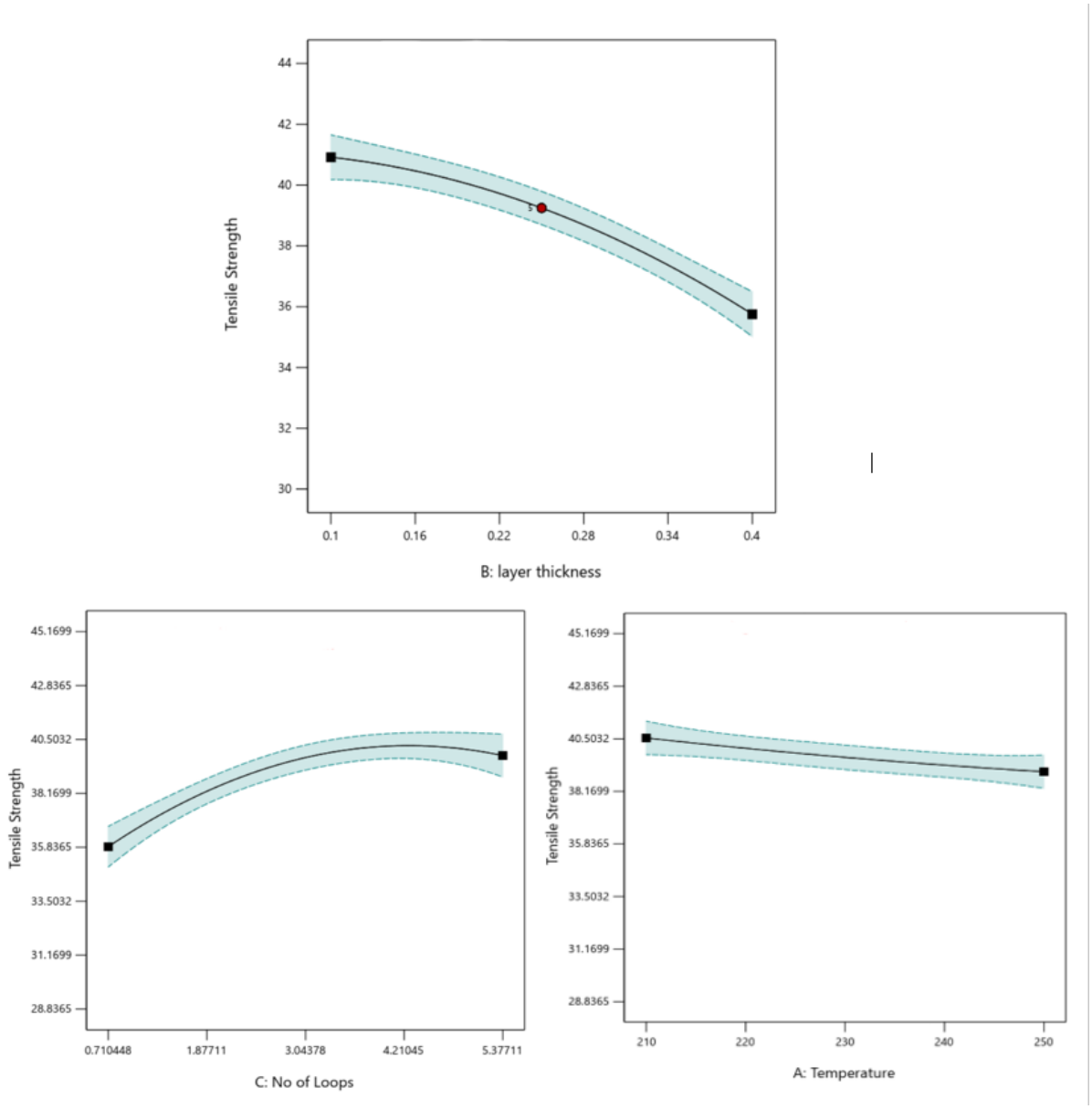

Fig. 27. Variation of tensile strength with respect to each input variable

CHAPTER 5: CONCLUSIONS

The analysis reveals crucial insights into the sensitivity of input variables in predicting the tensile strength of FDM fabricated components. Notably, Layer Thickness emerges as the most influential factor, followed by Temperature, while the impact of Number of Loops is relatively minimal. This underscores the critical importance of controlling layer thickness to achieve significant variations in tensile strength. Further examination through parametric analysis sheds light on the relative importance of model inputs and elucidates how tensile strength fluctuates with changes in input variables. For instance, there's a discernible decrease in tensile strength with increasing layer thickness and conversely, an increase with the number of loops. Additionally, it unveils a parabolic non-linear relationship between tensile strength and both the number of loops and layer thickness.

Drawing from these insights, optimal values of input variables can be discerned to optimize tensile strength. This empowers our proposed model to offer valuable insights into the impact of input process parameters on tensile strength, facilitating informed decision-making in component fabrication processes. In conclusion, our project has contributed to a comprehensive understanding of the FDM process and its correlation with Tensile Strength, particularly emphasizing the influences of Extruder Temperature, number of contours, and Layer Thickness in 3D printing.

Through meticulous experimentation and robust data analysis, our project has successfully developed a Machine Learning (ML) model tailored for predicting tensile strength and optimizing process parameters in extrusion manufacturing, with Support Vector Regression (SVR) emerging as the preferred choice. SVR's superiority over the widely used Artificial Neural Network (ANN) model is evidenced by its lower Mean Squared Error (MSE) and higher R-squared value, indicating heightened accuracy and stronger correlation between input parameters and tensile strength. Additionally, SVR's adeptness in handling non-linear relationships, outliers, computational efficiency, and interpretability further solidify its position as the optimal choice, ultimately advancing the understanding and application of ML in extrusion manufacturing, thereby enhancing product quality and performance in FDM-based manufacturing processes.

APPENDIX

SVR CODE:

```
{
import pandas as pd
from sklearn.model_selection import train_test_split, GridSearchCV
from sklearn.preprocessing import StandardScaler
from sklearn.svm import SVR
from sklearn.metrics import mean_squared_error
from sklearn.metrics import r2_score # Import r2_score
from joblib import dump

# Read data from Excel file
data = pd.read_excel('data.xlsx')

# Separate features (X) and target variable (y)
X = data.iloc[:, :-1] # all columns except the last one
y = data.iloc[:, -1]  # last column

# Split data into training and testing sets
X_train, X_test, y_train, y_test = train_test_split(X, y, test_size=0.3,
random_state=42)

# Standardize features
scaler = StandardScaler()
X_train_scaled = scaler.fit_transform(X_train)
X_test_scaled = scaler.transform(X_test)

# Define parameter grid
param_grid = {
  'C': [0.1, 1, 10],          # Regularization parameter
  'gamma': ['scale', 'auto'],     # Kernel coefficient
  'kernel': ['rbf', 'linear']     # Kernel type
}

# Initialize SVR
svr = SVR()

# Perform Grid Search Cross-Validation
grid_search = GridSearchCV(svr, param_grid, cv=5,
scoring='neg_mean_squared_error')
grid_search.fit(X_train_scaled, y_train)
```

```
# Get the best model
best_svr_model = grid_search.best_estimator_

# Save the best model
dump(best_svr_model, 'best_svr_model.joblib')

# Make predictions on the testing set
y_pred = best_svr_model.predict(X_test_scaled)

# Calculate Mean Squared Error (MSE)
mse = mean_squared_error(y_test, y_pred)
print("Mean Squared Error:", mse)

# Calculate R-squared value
r2 = r2_score(y_test, y_pred)
print("R-squared:", r2)

# Comparing predicted and experimental values
comparison_df = pd.DataFrame({'Experimental': y_test, 'Predicted':
y_pred})
print("\nExperimental vs. Predicted Values:")
print(comparison_df)

# Print best parameters
print("Best Parameters:", grid_search.best_params_
}
```

ANN CODE:

```
{
import pandas as pd
from tensorflow import keras
from tensorflow.keras import layers
from kerastuner.tuners import Hyperband
from tensorflow.keras.callbacks import ModelCheckpoint
import tensorflow.keras.backend as K  # Import Keras backend
from sklearn.metrics import r2_score

# Load data from Excel file
df = pd.read_excel('data.xlsx')

# Separate independent and dependent features
```

```
X = df.iloc[:, :-1] # Independent features
y = df.iloc[:, -1]  # Dependent feature


# Define the function to build the model
def build_model(hp):
  model = keras.Sequential()
   for i in range(hp.Int('num_layers', 1, 20)):
# Vary number of layers from 2 to 40
    units = hp.Int(f'units_layer_{i}', min_value=2, max_value=1000,
step=32)
    model.add(layers.Dense(units=units, activation='sigmoid'))
# Change activation to sigmoid
  model.add(layers.Dense(1, activation='linear')) # Output layer
  model.compile(
    optimizer=keras.optimizers.Adam(hp.Choice('learning_rate', [1e-2,
1e-3, 1e-4, 7e-1, 7e-2])),
    loss='mean_squared_error',
    metrics=['mean_squared_error'])
  return model

# Initialize Hyperband tuner
tuner = Hyperband(
  build_model,
  max_epochs=20,  # Set the maximum number of epochs
  objective='val_mean_squared_error',
  factor=3, # Reduction factor for the number of epochs and number of
models
  directory='project',
  project_name='ANN_Search',
  overwrite=True) # Overwrite existing project

# Define checkpoint callback to save the best model in .h5 format
checkpoint_callback = ModelCheckpoint(filepath='best_model-
sigmoid.keras',
                      monitor='val_mean_squared_error',
                      save_best_only=True,
                      verbose=1,
                      mode='min', # Set mode to 'min' if monitoring loss
                      save_weights_only=False) # Save the entire model

# Perform the hyperparameter search
tuner.search(X, y,
```

```
        epochs=1000, # Set the number of epochs for each trial
        validation_split=0.3, # Set the validation split
        callbacks=[checkpoint_callback]) # Add the checkpoint
callback

# Get the best hyperparameters
best_hps = tuner.get_best_hyperparameters(num_trials=1)[0]

# Print the best combination of layers and neurons
best_combination = {}
for key, value in best_hps.values.items():
  if 'units_layer_' in key:
    layer_index = int(key.split('_')[2])
    best_combination[layer_index] = value
print("Best combination of layers and neurons:", best_combination)
best_model = tuner.get_best_models(num_models=1)[0]

# Evaluate the best model on the test data
y_pred = best_model.predict(X)
r2 = r2_score(y, y_pred)
print("R-squared for the best model:", r2)
}
```

Table. 11: Prediction of tensile strength for some of the combinations

Temperature (C)	Layer Thickness (mm)	No of Loops	Predicted Output (MPa)
210	0.1	1	38.11000795
210	0.1	2	38.50778467
210	0.1	3	38.9055614
210	0.1	4	39.30333812
210	0.1	5	37.54469948
210	0.11	1	37.94247621
210	0.11	2	38.34025293
210	0.11	3	38.73802966
210	0.11	4	39.13580638
210	0.11	5	37.37716774
210	0.12	1	37.77494447
210	0.12	2	38.17272119
210	0.12	3	38.57049792

210	0.12	4	38.96827465
210	0.12	5	37.209636
210	0.13	1	37.60741273
210	0.13	2	38.00518946
210	0.13	3	38.40296618
210	0.13	4	38.80074291
210	0.13	5	37.04210427
210	0.14	1	37.43988099
210	0.14	2	37.83765772
210	0.14	3	38.23543444
210	0.14	4	38.63321117
210	0.14	5	36.87457253
210	0.15	1	37.27234925
210	0.15	2	37.67012598
210	0.15	3	38.0679027
210	0.15	4	38.46567943

REFRENCES

1. Jayanth, N., Senthil, P., & Prakash, C. (2018). "Effect of chemical treatment on tensile strength and surface roughness of 3D-printed ABS using the FDM process."

2. Syrlybayev, D., Zharylkassyn, B., Seisekulova, A., Akhmetov, M., Perveen, A., & Talamona, D. (2021, May 14). "Optimisation of Strength Properties of FDM Printed Parts—A Critical Review."

3. Shirmohammadi, M., Jafarzadeh, S., & Keshtiban, P. M. (2021). "Optimization of 3D printing process parameters to minimize surface roughness with hybrid artificial neural network model and particle swarm algorithm."

4. Wagari Gebisa, A., & Lemu, H. G. (2018). "Influence of 3D Printing FDM Process Parameter on Tensile Property of ULTEM 9085."

5. Singh, G., Missiaen, J. M., Bouvard, D., & Chaix, J. M. (2021). "Copper extrusion 3D printing using metal injection moulding feedstock: Analysis of process parameters for green density and surface roughness optimization."

6. Yang, L., Li, S., Li, Y., Yang, M., & Yuan, Q. (2019). "Experimental Investigations for Optimizing the Extrusion Parameters on FDM PLA Printed Parts."

7. Yadava, D., Chhabra, D., Garg, R. K., Ahlawat, A., & Phogat, A. (2020). "Optimization of FDM 3D printing process parameters for multi-material using artificial neural network."

8. Lalegani Dezaki, M., Anuar, M. K., Serjouei, A. Z., Hatami, S., & Bodaghi, M. (2021). "Influence of Infill Patterns Generated by CAD and FDM 3D Printer on Surface Roughness and Tensile Strength Properties."

9. Shirmohammadi, M., Goushchi, S. J., & Keshtiban, P. M. (2021). "Optimization of 3D printing process parameters to minimize surface roughness with hybrid artificial neural network model and particle swarm algorithm."

10. Mengesha Medibew, T. (2022). "A Comprehensive Review on the Optimization of the Fused Deposition Modeling Process Parameter for Better Tensile Strength of PLA-Printed Parts."

11. Mani, M., Karthikeyan, A. G., Kalaiselvan, K., Muthusamy, P., & Muruganandhan, P. (2022). "Optimization of FDM 3-D printer process parameters for surface roughness and mechanical properties using PLA material."

12. Giri, J., Shahane, P., Jachak, S., Chadge, R., & Giri, P. (2021). "Optimization of FDM process parameters for dual extruder 3d printer using Artificial Neural network."

13. Jatti, V. S., Sapre, M. S., Jatti, A. V., Khedkar, N. K., & Jatti, V. S. (2022). "Mechanical Properties of 3D-Printed Components Using Fused Deposition Modeling: Optimization Using the Desirability Approach and Machine Learning Regressor."

14. Diriba Tura, A., Mamo, H. B., & Gemechu, W. F. (2021). "Mathematical modeling and parametric optimization of surface roughness for evaluating the effects of fused deposition modeling process parameters on ABS material."

15. Rajpurohit, S. R., & Dave, H. K. (2020). "Impact strength of 3D printed PLA using open source FFF based 3D printer."

16. Roberson, D. A., Perez, A. R. T., Shemelyaa, C. M., Rivera, A., & MacDonalda, E. (Year). "Comparison of stress concentrator fabrication for 3D printed polymeric izod impact test specimens."

17. Raut, N. P., & Kolekar, A. B. (2022). "Experimental analysis of 3D printed specimens with different printing parameters for Izod impact strength."

18. Rajpurohit, S. R., & Dave, H. K. (2021). "Impact strength of 3D printed PLA using open source FFF-based 3D printer."

19. Atakok, G., Kam, M., & Koc, H. B. (2022). "Tensile, three-point bending and impact strength of 3D printed parts using PLA and recycled PLA filaments: A statistical investigation."

20. "About ABS." (Acrylonitrile Butadiene Styrene (ABS Plastic): Uses, Properties & Structure) Retrieved from specialchem.com.

21. "About Additive Manufacturing." (What is Additive Manufacturing | GE Additive) Retrieved from ge.com.

22. "Uses of Additive Manufacturing." (5 Unstoppable Industries Using Additive Manufacturing | Stratasys Direct) Retrieved from stratasysdirect.com.
23. Fish Bone diagram available at : https://www.researchgate.net/figure/A-fishbone-diagram-to-illustrate-the-main-effect-of-process-parameters-on-FDM-FFF-part_fig1_355474796

24. Sample image of FDM available at: https://www.allthat3d.com/fdm-3d-printing/

25. Airbus Takes on Stratasys 3D Printing for Serial Part Production :https://www.engineering.com/story/airbus-takes-on-stratasys-3d-printing-for-serial-part-production

26. Medical 3D printing applications uploaded by Amit Arefin: https://www.researchgate.net/figure/Medical-3D-printing-applications-for-A-spinal-fusion-cage-95-B-dental-model-96_fig4_351366436

27. Uses of FDM in military available at: https://www.alamy.com/soldier-artificial-prosthetic-limb-hand-war-veteran-image430842434.html

28. Comprehensive Guide on Acrylonitrile Butadiene Styrene (ABS): https://omnexus.specialchem.com/selection-guide/acrylonitrile-butadiene-styrene-abs-plastic

29. Agatonovic-Kustrin, S., & Beresford, R. (1999). "Basic Concepts of Artificial Neural Network (ANN) Modeling and Its Application in Pharmaceutical Research."

30. Vijayaraghavan, V., Garg, A., Lam, J. S. L., Panda, B., & Mahapatra, S. S. (2014). "Process Characterisation of 3D-Printed FDM Components Using Improved Evolutionary Computational Approach."

31. Analytics Vidhya. (2020). "Support Vector Regression Tutorial for Machine Learning." Retrieved from https://www.analyticsvidhya.com/blog/2020/03/support-vector-regression-tutorial-for-machine-learning/.

32. ResearchGate. (n.d.). "A Schematic Diagram of the Support Vector Regression Using ε-Sensitive. https://www.researchgate.net/publication/26543790/figure/fig1/AS:310045121236994@1450931925958/A-schematic-diagram-of-the-support-vector-regression-using-e-sensitive-loss-function.png.